JBC Papers in Press. Published on October 29, 2002 as Manuscript M210360200

Spectroscopic Observations of Ferric Enterobactin Transport

Zhenghua Cao, Paul Warfel, Salete M.C. Newton, and Phillip E. Klebba*

Department of Chemistry & Biochemistry

University of Oklahoma

Norman, OK 73019

Running title: Fluorescence spectroscopy *in vivo*

*Corresponding author: peklebba@ou.edu

ABSTRACT

We characterized the uptake of ferric enterobactin (FeEnt), the native *E. coli* ferric siderophore, through its cognate outer membrane receptor protein, FepA, using a site-directed fluorescence methodology. The experiments first defined locations in FepA that were accessible to covalent modification with fluorescein maleimide (FM) *in vivo*: among 10 sites that we tested by substituting single Cys residues, FM labeled W101C, S271C, F329C and S397C, and all these exist within surface-exposed loops of the OM protein. FeEnt normally adsorbed to the fluoresceinated S271C and S397C mutant FepA proteins *in vivo*, which we observed as quenching of fluorescence intensity, but the ferric siderophore did not bind to the FM-modified derivatives of W101C or F329C. These *in vivo* fluorescence determinations showed, for the first time, consistency with radioisotopic measurements of the affinity of the FeEnt-FepA interaction: K_d was 0.2 nM by both methods. Analysis of the FepA mutants with AlexaFluor$_{680}$, a fluorescein derivative with red-shifted absorption and emission spectra that do not overlap the absorbance spectrum of FeEnt, refuted the possibility that the fluorescence quenching resulted from resonance energy transfer. These and other data instead indicated that the quenching originated from changes in the environment of the fluor, as a result of loop conformational changes during ligand binding and transport. We used the fluorescence system to monitor FeEnt uptake by live bacteria, and determined its dependence on ligand concentration, temperature, pH and carbon sources, and its susceptibility to inhibition by the metabolic poisons. Unlike cyanocobalamin transport through the OM, FeEnt uptake was sensitive to inhibitors of electron transport and phosphorylation, in addition to its sensitivity to proton motive force depletion.

INTRODUCTION

Gram-negative bacteria recognize and transport a variety of ferric siderophores (1, 2) through outer membrane (OM) receptor proteins that function as ligand-gated porins (LGP; 3). Some of the hallmarks of these transport processes are the specificity with which LGP select their iron-containing ligands (4-7), the high affinity of the receptor-ligand interactions (8, 9), conformational changes in the receptors during ligand binding (10-13) and transport (14, 15), the requirement for the accessory proteins TonB (16), ExbB and ExbD (17, 18), and the need for cellular energy to accomplish active transport of the their metal-containing ligands through the OM (19-22). This latter energy requirement is atypical in a bilayer that contains open channels (23-26), and therefore cannot sustain an ion gradient. At present the pathways through which both energy and TonB participate in metal transport are unresolved (27-29). The crystal structures of FepA (30), FhuA (31, 32) and FecA (13) revealed that their N-terminal 150 amino acids fold into a 4-stranded $-sheet domain that lodges within otherwise typical transmembrane $-barrels, creating a third mechanistic paradox: how do ligands pass through such closed pores?

Site-directed biophysical methodologies defined many of the biochemical properties of FepA (10, 11, 14, 33), by derivatization of the genetically engineered mutant FepAE280C with fluorescent or paramagnetic labels. Residue E280C exists on the external surface of the receptor's 3rd surface loop (L3) (33, 30), and nitroxide spin labels attached to it reflected structural changes in FepA when FeEnt binds, and different motion when it passes through the OM protein (14). Similarly, the binding of either FeEnt or ColB quenched fluorescein labels attached to purified FepAE280C, which allowed determination of the thermodynamic and kinetic properties of the binding reaction (10, 11). One of the conspicuous findings of those experiments was that purification reduced the affinity of FepA for FeEnt (9, 10), and the affinity

of FhuA for its ligand, ferrichrome (35, 7), at least 100-fold. In this report we applied fluorescence methodologies to FeEnt transport *in vivo*: the sensitivity and specificity of the technique provided not only an explanation for the discrepancies in affinity that were observed *in vivo* and *in vitro*, but more detailed information on the ligand internalization reaction through the OM, including its temperature, pH, and energy dependence.

METHODS

Bacterial strains, plasmids and chemicals. *E. coli* K12 strains KDF541 (*F*$^-$, *thi, entA, pro, trp, rpsL, recA, fepA, fhuA, cir;* 3) and KDF571 (KDF541, but *tonB*; 3) were hosts for *fepA*$^+$ pUC19 derivatives pITS449 (36) and pT944 (11). Both plasmids encode wild type FepA, but pT944 contains a series of genetically engineered restriction sites that facilitate cloning procedures and restriction fragment exchange. pMF19 (37; provided by M.A. Valvano) is a pEXT21-derivative that carries *wbbL*, the structural gene for a rhamnosyltransferase involved in O16 LPS biosynthesis. Fluorescent reagents were purchased from Molecular Probes.

Ferric enterobactin. Enterobactin was purified from *E. coli* strain AN102 (39), and FeEnt was prepared and purified as previously described (40); its concentration was determined from absorbance at 495nm ($_{495nm}$ = 5.6 ; 41).

Anti-Iodoacetamide-fluorescein (IAF) sera. Rabbits were immunized weekly for one month with 5-IAF (Molecular Probes) conjugated to bovine serum albumin (BSA), and subsequently bled through the ear. Sera were titered by ELISA (> 10,000) and western immunoblot against ovalbumin-IAF conjugates.

Site-directed mutagenesis. We used QuikChange (Stratagene) for site-directed mutagenesis (7, 12) on pITS449 or pT944, and designated the mutant FepA proteins FepAXnY, where X represents the one-letter abbreviation for the wild type residue at position n, and Y represents the one-letter abbreviation for the substituted amino acid.

We tested the functionality of each FepA mutant by evaluating its expression (42), susceptibility to colicins B and D (40), ^{59}FeEnt binding (9) and FeEnt transport in qualitative siderophore nutrition assays (5) and quantitative determinations of ^{59}FeEnt uptake (9).

Fluorescence labeling of live cells. For fluorescein labeling of live bacteria, we grew the cells to stationary phase in LB broth (43) and subcultured at 1% into MOPS media (44) containing appropriate nutritional supplements, at 37 ^{o}C with shaking, to mid-log phase. For labeling in energy-deficient conditions, after growth in LB and subculture in MOPS the bacteria were collected by centrifugation and resuspended in the same volume of MOPS media, but without glucose, casamino acids, and with half the usual supplementation of required amino acids. The culture was then incubated with shaking for 10 hrs at 37 ^{o}C.

Bacteria were collected by centrifugation (5000 x g, 20 min), washed with and resuspended in Tris-buffered saline (TBS), pH7.4, to a final concentration of 5 x 10^{8} cells/ml. Fluorescein maleimide (FM) or AlexaFluor$_{680}$ maleimide (AM) in dimethyl formamide (less than 0.1% of final volume), was added to a final concentration of 5 uM, and incubated at room temperature for 30 minutes in the dark, with shaking. The labeled cells were centrifuged, washed 3 times with 25 ml of ice-cold TBS plus 0.05% Tween-20, washed once with and resuspended in ice-cold TBS, and stored on ice for immediate use.

Labeling specificity. We evaluated labeling specificity with anti-FepA and anti-IAF immunoblots of cell lysates, and by fluorescence emission scans of labeled experimental and control bacterial cultures. In the former case, lysates from 10^8 cells were subjected to 10% SDS-PAGE and western immunoblot with anti-BSA-IAF sera; the reactions were quantified on a Storm Scanner (Molecular Dynamics) after development with ^{125}I-protein A (42). The immunoblots showed that expression of FepA did not significantly vary under the culture conditions we employed. The anti-BSA-IAF serum was equally effective against proteins and cells modified by (FM), demonstrating its recognition of the fluorescein moiety.

Fluorescein's characteristic orange color facilitated qualitative evaluation of labeling specificity by visual inspection of treated cell pellets. Strains expressing wild type FepA, which was not labeled by either IAF or FM, were not colored after treatment with the reagents, whereas bacteria expressing mutant FepA proteins containing single, genetically engineered cysteines in accessible locations were identified by the orange color of their cell pellets. To quantitatively determine fluorescein labeling specificity, we performed emission scans at 20^{o}C, with an excitation wavelength of 490nm and a 5 s integration time. We compared scans for fluorescein-labeled strains expressing wild type and mutant FepA proteins, and used scans of untreated bacteria to establish the background fluorescence.

Fluorescence measurements. Using an SLM 8000 fluorimeter (Rochester, NY), upgraded to 8100 functionality, we recorded the fluorescence intensities of bacteria (5 x 10^7 cells) suspended in 2 ml of either TBS or MOPS media, and equilibrated at temperature. For fluorescence determinations of FeEnt binding affinity, we added various concentrations of FeEnt to the cell suspension and recorded fluorescence intensity with excitation and emission wavelengths of

490nm and 518nm, respectively, for fluorescein, and 679 nm and 702 nm for AlexaFluor$_{680}$. We accounted for background fluorescence and volume changes, and analyzed the data with the bound (1-F/F$_0$) vs total (FeEnt) function of GraFit 4 (*Erithacus*, Middlesex, UK).

Effects of energy inhibitors on FeEnt transport. To study the effect of inhibitors on FeEnt uptake, 5 x 10^7 FM-labeled, energy-starved cells were first incubated for 60 min at 37^{o}C with shaking, in TBS buffer plus glucose (0.4%) and the corresponding inhibitors. The cells were transferred to the sample cuvette, equilibrated at the measurement temperature, and the uptake time course was recorded.

RESULTS

Site-directed covalent modification with fluorescein maleimide *in vivo*: effect of lipopolysaccharide. OM proteins contain few unpaired cysteines, and we tested the possibility that genetically engineering single Cys residues at sites of interest may be covalently modified in live bacteria with –SH specific fluorescent probes. Although we previously modified residue E280C in FepA L3 with nitroxide compounds (33, 34, 14), we could not label it with fluorescent probes (45), probably because of the inaccessibility of sites close to the hydrophilic OM surface to hydrophobic molecules like fluorescein (Fig. 1A). Therefore, from the FepA crystal structure we designed and introduced 10 more individual, unpaired Cys residues at positions either on the cell surface, or within the periplasm: W101C, S150C, S211C, Y260C, S271C, F329C, S397C, S423C, S575C, and S595C. Among these 10 target Cys residues, FM specifically labeled W101C, S271C, F329C and S397C, which all reside in cell surface-exposed loops of FepA (Fig. 1A), above the level of the LPS core sugars: W101 lies in the second loop of

the N-domain, while S271, F329 and S397 exist in loops 3, 4 and 5, respectively, of the C-domain. FM also specifically modified, at lower levels, sites S63C and S150C, which reside in NL1 and on the periplasmic rim of the FepA $-barrel, respectively .

Further study showed that two circumstances affected the specificity and efficiency of the fluorescence labeling procedure: the nature of the LPS O-antigen, and the bacterial culture conditions. In our initial experiments the bacteria adsorbed fluorescence probes, but we saw little difference in the fluorescence intensity of FM-treated KDF541/pFepAS271C and Kdf541/pITS449 (*fepA+).* The use of two different reagents, IAEDANS and coumarin maleimide, did not remedy this lack of specificity (data not shown). The *E. coli* strain that was the usual host for plasmids, KDF541, produces rough LPS, without any O-antigen, and we considered the possibility that LPS was a determining factor in the specificity of the fluorescence labeling reactions. The use of deep rough mutants strains did not improve the labeling specificity of surface-exposed Cys residues (data not shown). Although western blots revealed specific covalent modification of some of the Cys mutants, FM non-specifically adsorbed to deep rough strains, which was apparent in the yellow color of the cell pellets, that was not diminished by repeated washing. These results suggested that in deep rough strains, and to a lesser extent in rough strains, the fluorescent reagents penetrated into the OM bilayer and resisted washing procedures. The converse experiment confirmed this inference: the use of bacterial cells synthesizing full length LPS minimized non-specific adsorption of fluorescent dyes. We achieved this result by introducing pMF19, which carries a rhammnosyl transferase that allows production of the LPS O-chain (wbbL$^+$; 37*).* Strains harboring pMF19 and one of the four accessible Cys substitution mutants of FepA were specifically labeled by FM, as seen by fluorescence intensity measurements of live bacteria, and in western immunoblots (Fig. 1B).

FeEnt binding to fluorescein-labeled live bacteria. We measured the ability of the four surface-localized, Cys substitution mutants of FepA to bind ^{59}FeEnt, before and after fluoresceination. Adsorption of the ferric siderophore was weak and barely detectable in W101C- and F329C -FM; attachment of fluorescein at these sites sterically hindered the adsorption of the siderophore. These data concurred with the prior conclusion that residue F329 exists in close proximity to, or is a component of, an initial FeEnt binding site (B1; 11); the crystal structure shows W101C in the middle of the FepA vestibule (Fig. 1A). On the other hand, FM-modification of S271C or S397C did not interfere with FeEnt recognition and binding: bacteria expressing either of these mutant proteins manifested normal (sub-nanomolar) binding affinities (Fig. 2), even after fluoresceination. These experiments showed, for the first time, exact correspondence between the binding affinities measured *in vivo,* by radioisotopic and fluorescence methodologies (K_d = 0.2 nM). In subsequent experiments we exclusively studied the S271C site, located at the extremity of L3.

FeEnt binding to Alexa Fluor$_{680}$-labeled bacteria. Ligand binding diminishes the fluorescence of probes attached to FepA at E280C, and our modifications and analyzes of S271C and S397C showed the same quenching phenomenon *in vivo.* Previous determinations of binding kinetics found a biphasic association reaction between purified FepAE280C-FM and FeEnt, and ColB (10, 11). We interpreted these data as initial ligand adsorption to an external site (B1), followed by movement to a second site, deeper in the vestibule (B2). The ability of E280C-FM to reflect these two binding phases presumably arose from changes in the local environment of the fluor, that occurred as the receptor protein underwent conformational dynamics during ligand adsorption. However, because its absorption spectrum overlaps the

emission spectrum of fluorescein, the possibility existed that during its binding FeEnt quenched fluorescence by energy transfer between the excited fluor and the ferric siderophore. Studies with a red-shifted fluorescein derivative that does not overlap the absorption spectrum of FeEnt [AlexaFluor$_{680}$ (AM): 679 nm and 702 nm, respectively], refuted this explanation (Fig. 2): during FeEnt binding, FepA proteins modified with AM exhibited equivalent reductions in intensity to those modified with FM. The comparable quenching of AM, without the possibility of energy transfer to FeEnt, indicated that the reductions in intensity did not derive from close proximity of the ferric siderophore to the fluor. Rather, the data favored the notion that binding triggers conformational dynamics that alter the environment of the reporter molecules.

Temperature dependent changes in polarization. At physiological temperatures we expected a decrease in the polarization of fluorescent labels attached to the surface loops of FepA, because of increased Brownian motion (46, 47). The polarization of FepAS397C-FM (in L5) decreased as the temperature of the system raised, but that of FepAS271C-FM (in L3) increased (Fig. 3). These data confirmed that the temperature affected the motion of the attached fluor: L3 became less mobile, and L5 became more mobile, in response to increased temperature. These states were reversible, as the temperature of the system decreased again.

Fluorescence measurements of FeEnt uptake. When exposed to FeEnt at 20 ^{o}C, KDF541/pMF19/pS271C-FM bound and transported it, and we spectroscopically monitored these reactions. Subsequent to its binding, we observed FeEnt transport as a recovery of fluorescence intensity, but only when the extracellular free ligand was depleted by its uptake into the cells. At that time, when the population of receptor proteins was vacated, it's original

fluorescence intensity returned. The consumption of FeEnt was necessary to observe fluorescence changes, because when present, it bound and quenched again. Thus in the presence of sufficient excess of the ferric siderophore, we saw no renewal of fluorescence (15). When it occurred, the resurgence of fluorescence paralleled the kinetics of FeEnt uptake, independently measured in ^{59}Fe uptake experiments (Fig. 4). In those studies, the increase in fluorescence intensity occurred between 1200 and 1400 s. The corresponding radioisotope uptake experiment at 20 ^{o}C showed that accumulation of ^{59}FeEnt stopped at exactly the same time, as a result of depletion of the substrate from the media. So the recovery of fluorescence intensity precisely mirrored the depletion of the ligand from the culture.

Consistent with prior observations of the energy-dependent uptake reaction (9, 48, 49, 50, 51), the spectroscopic measurement of FeEnt transport was affected by media composition, FeEnt concentration and temperature. It occurred more slowly in bacteria deprived of nutritional requirements, either in minimal media lacking auxotrophic amino acid supplements, or suspended in TBS (Fig 5A). As discussed above, at 20 ^{o}C the transport of FeEnt was visible as a return of fluorescence intensity, and the concentration-dependence of the phenomenon was striking. For bacteria exposed to 2, 5, 10 and 20 nM FeEnt, the lag time preceding transport was 250, 550, 1000, and 2050 s, respectively (Fig. 5B). Furthermore, AM-labeled cells showed the same spectroscopic response as FM-labeled bacteria. These data indicated that the intensity changes that occurred during uptake also derived from conformational motion in the surface loops, in this case associated with ligand internalization. At 37 ^{o}C, in the presence of equimolar or sub-saturating FeEnt, the reaction occurred most rapidly (Fig. 5b inset), too rapidly to permit a detailed analysis. However, the fluorescence intensity changes were fully TonB-dependent, whether the experiments were conducted at 20 ^{o}C (Figure 5B) or 37 ^{o}C. A complete description

of the fluorescence changes associated with the 37 ^{o}C transport reaction, including its energy- and TonB-dependence, was given elsewhere (15).

The uptake reaction was pH-dependent. We attempted to study the process at pH 10, but found that FeEnt does not adsorb to FepA at high pH. This result concurred with the fact that basic residues [R286, 316 (42); K483 (12)] play a role in the binding of the acidic ferric siderophore. At pH 4 FeEnt bound and quenched the fluorescence intensity of KDF541/pMF19/pS271C-FM, but the magnitude of the quenching was slightly less, and the recovery of fluorescence that normally occurred as the temperature approached 37 ^{o}C did not take place at pH 4 (Fig. 5b), suggesting that uptake was impaired under these conditions.

We investigated the range of permissive temperatures for FeEnt uptake (Fig. 5c). As temperature decreased, so also did the slope of the fluorescence recovery. Conversely, the bacteria experienced a lag prior to the rebound of fluorescence increase, whose magnitude was inversely proportional to temperature. These data supported the conclusion that the recovery of fluorescence derived from the transport reaction. Somewhat unexpectedly, the bacteria transported FeEnt, although very slowly, even at 5^{o}C (Fig.5c).

Energy dependence and susceptibility to poisons. The proton ionophore CCCP, and the electron transport inhibitors cyanide and azide completely and indefinitely abrogated uptake of the ferric siderophore (Fig 6a); glucose starvation produced comparable effects (Fig. 6b). On the other hand, the proton ionophore DNP and the phosphate analog arsenate inhibited uptake, but not to the same extent: transport occurred in their presence, but the slope of the fluorescence increase was significantly reduced in both cases, such that the bacteria utilized the quantity extrinsic FeEnt (2 nM) in 1 or 2 hours, respectively; in the absence of inhibitors the cells

exhausted the exogenous ligand within 10 minutes. The effects of arsenate specifically related to its inhibition of phosphate metabolism, because the presence of 30 mM phosphate effectively suppressed arsenate inhibition (Fig. 6c). Finally, in the absence of glucose, ascorbic acid and succinate effectively restored transport activity, although in the latter only supported transport at a much slower rate.

DISCUSSION

Variations in the fluorescence intensity of bacteria labeled with fluorescein or AlexaFluor$_{680}$ at FepA residue S271C reflected the active transport of FeEnt through the OM layer of the cell envelope. The spectroscopic phenomena recapitulated the characteristics of the energy dependent active transport reaction: high affinity, occurring at concentrations as less than 2 nM; a direct relationship between lag time and initial ligand concentration; temperature-dependence of the rate of intensity change; consistency with uptake measurements by radioisotopic determinations; susceptibility to energy poisons. These data unambiguously demonstrate that the recovery of fluorescence after FeEnt binding originates from its uptake reaction through the OM. The spectroscopic system offers an alternative to existing methods for observation of OM transport, that is sensitive, precise, continuous, and amenable to quantitative analysis.

The evidence that the fluorescence measurements describe conformational motion during the uptake reaction stems from several independent observations. (i) In prior work utilizing FepAE280C-FM, we concluded that conformational change occurs in L3 *in vitro*, because the modified side chain of E280C resides on the outside of the surface vestibule, where it cannot contact FeEnt, and similar quenching was engendered by binding of colicin B, which contains no metal complex. These data made collisional quenching unlikely for either ligand, and

excluded energy transfer as a mechanism to explain the effects of ColB, which has no chromophores. (ii) In the current experiments, the FepA crystal structure suggests that fluorescein attached to S271C, at the extremity of L3, likely projects toward the interior of the vestibule. The observation that FeEnt binding quenches S271C-AM in the same way that it quenches S271C-FM eliminates energy transfer as an explanation of the inhibition. (iii) These data do not rule out collisional quenching of fluors attached to S271C, but this possibility seems unlikely. Modification of S271C with fluorescein had no effects on the affinity, capacity or transport of ^{59}FeEnt, indicating that this residue does not likely contact FeEnt during binding or uptake. Fluoresceination of F329, on the other hand, abrogated FeEnt adsorption and transport (45) reinforcing this inference. In addition, (iv) given the extensive spectral overlap of FeEnt and fluorescein, it seems unlikely that significant collisional quenching can occur without significant energy transfer, which was not found. (v) From a logistic perspective, FeEnt binds to the outside of a closed channel, so some sort of conformational change is necessary to promote its internalization. Finally, (vi) the loops of FepA (L7; 12) and FecA (L7 and L8; 13) are conformationally active during FeEnt binding, and loop motion was previously seen *in vivo* (14). In summary, a body of evidence argues against either collisional or energy transfer mechanisms of quenching, leaving conformational dynamics that relocalize the flour to a quenching environment as a single viable explanation for the quenching phenomena. This conclusion concurs with data acquired by a variety of methodologies (7, 10, 12, 13, 14, 32, 33, 34).

Because L3, L5 and L7 in FepA change in conformation during the interaction with ligand, it appears likely that such motion is a general property of LGP surface loops. We envision a model of FepA conformation in which the receptor exists in an extended, open form

in the absence of ligand, but closes around ligands when they bind. At either 4 ^{o}C or 20 ^{o}C FeEnt adsorption creates the closed state, in which the fluor undergoes maximal quenching from increased collisions with water or other polar or charged molecules, in the environment created by the aggregation of the loops around the ligand. This mechanism agrees with the observation of biphasic binding kinetics for ligand adsorption to FepA, and with contractions from open to closed states of FecA loops 7 and 8, and FepA L7. As the temperature warms and FepA transports FeEnt, fluorescence rebounds, because the now empty receptor proteins revert from the closed state to the open state. At 37 ^{o}C, further motion occurs that results in additional quenching (18).

One perplexing finding about FepA and FhuA was that purification from the OM quite drastically decreased their ability to bind ligands. This decrease questioned the relevance of the crystallographic data to the structures of the siderophore receptors *in vivo.* However, two different techniques, ^{59}FeEnt binding *in vivo* (9) and fluorescence spectroscopy *in vitro* (10), defined the discrepancy, raising the possibility of methodological bias. The results we report eliminate this contingency, by determining with a fluorescence methodology that the affinity of FepA for FeEnt in live bacteria is in fact sub-nanomolar: K_d = 0.1 -0.2 *n*M, as now established by two independent methods. Thus these data confirm that extraction from the OM reduces the affinity of FepA for FeEnt about 100-fold [K_d = 10 nM (10)]. Furthermore, the affinity of native FepA for FeEnt *in* vivo is 20,000–fold greater than that of the isolated FepA N-domain *in vitro* [K_d = 5 uM (52)]. The upshot of these considerations is that at the K_d measured *in vivo*, purified FepA is less than 1% saturated with FeEnt, but why? The crystal structures of both ligand-free and ligand-bound FepA and FhuA revealed a closed form of the proteins, with loops condensed together above the membrane channel, whereas later crystallographic and

crosslinking studies *in vivo* showed that the loops may extend into an open conformation. Thus, the likely explanation for the discrepancy in binding affinities between the native and purified receptors is that in the former environment, in the absence of ligands, LGP adopt an open conformation, but when complexed with a ferric siderophore, or removed from the OM, their loops close.

Besides its prior application to the binding reactions between FepA and its ligands, site-directed fluorescence spectroscopy defined conformational changes in FhuA L5 during ferrichrome binding (53). The intrinsic fluorescence of pyoverdin, furthermore, facilitated characterization of its adsorption to the pseudomonad OM protein, FpvA (54-56). Our experiments are the first to use site-directed fluorescence to directly observe protein motion associated with uptake of a ligand through a membrane. It's important to note that the methodology does not necessarily reflect exclusively OM transport. Although the intensity changes in fluors attached to FepA derive from fluctuations of its loops between open and closed states, we only observed the recovery of fluorescence when the exogenous ligand was completely exhausted. In our experiments the bacteria had an ^{59}FeEnt binding capacity of 80 *p*Mol/10^9 cells (data not shown): when we provided 10 nM FeEnt in the medium, the 2.5 x 10^7 cells/ml underwent 5 rounds of transport to fully deplete the external ferric siderophore. This quantity of FeEnt exceeds the concentration of FepB in the periplasm (57), so its complete utilization by the bacteria requires transport through the inner membrane to the cytoplasm.

On the other hand, 2 nM FeEnt, the amount that we employed to study the susceptibility of the fluorescence phenomena to energy inhibitors, is a concentration that precisely saturates the bacteria. Therefore, its depletion from the media involves only a single round of transport by the FepA proteins of the OM, without requirement for uptake through the inner membrane. The

fact that we saw an immediate recovery of fluorescence, without a lag period, when we provided 2 nM FeEnt, supports this inference. At this stoichiometric concentration, the assay exclusively measured the activity of the OM component. The ability to monitor OM transport, without the need for null mutants in the subsequent, IM permease components (i.e., *fepC, fepD* or *fepG),* is a significant advantage of the spectroscopic approach. Our characterization of the energetics of the OM transport stage diverged from those obtained for cyanocobalamin uptake (21, 22), in that inhibitors of electron transport (cyanide and azide), phosphorylation (arsenate) and proton motive force (CCCP and DNP) all impaired FeEnt uptake through FepA, in some cases abrogating transport. In the vitamin B12 transport system, DNP-mediated depletion of PMF inhibited OM transport, but the process was insensitive to cyanide. Bradbeer conducted those experiments by radioisotopic methods in an *atp* genetic background (22, 38), whereas our strains were atp^+. Most other considerations were similar between his experiments and ours, except the pre-incubation times of the bacteria with the poisons, which were 10 min (22) and 40 min (this report). Our data almost exactly reprise, nevertheless, a prior characterization of the energy dependence of FeEnt uptake by *E. coli* (58), that was performed by radioisotopic methods. The explanation of these differences and similarities awaits further experimentation.

Figure legends

Figure 1. Accessibility of cysteine substitution mutants to fluorescein labeling *in vivo*. A. We engineered ten cysteine substitutions in pITS449 ($fepA^+$ on pUC18), expressed them in KDF541/pMF19 in MOPS minimal media, and labeled them with FM. The structural model (30) shows the Cys substitutions relative to the OM bilayer, and to the position of LPS (32) associated with the exterior of the FepA $-barrel. The N-domain

backbone is colored red, the $-barrel backbone is green; the sites of mutation and LPS, in space-filling format, are shown in CPK colors. The positions of residues S271 and F329, which were not defined in the crystal structure, are only estimated, as delimited by the last solved residues of L3 (orange: G323, Q335) and L4 (red: A383, D400) respectively. **B.** After fluorescent labeling, 10^8 labeled cells were lysed and subjected to western immunoblot with anti-BSA-IAF, developed with ^{125}I-protein A.

Figure 2. **Ligand binding by fluorescein-labeled FepA.** KDF541 expressing S271C (○) or S397C (●) and labeled with FM was diluted to 2.5 x 10^6/ml in TBS buffer, and fluorescence intensity was measured in the presence of varying amounts of FeEnt. KDF541 expressing wildtype FepA was subjected to the same procedure and used as a control for non-specific adsorption of FM. After background and dilution correction, 1-F/F_0 was fit against the FeEnt concentration, using GraFit 4 (Erithacus, Middlesex, UK), "Bound vs Total" equation. The Kd values for FepAS271C and FepAS397C were 0.263 nM (std. error 0.032 nM) and 0.292 nM (0.021 nM), respectively. The inset shows the ability of FeEnt (added at 200 s) to quench the fluorescence of cells labeled with AM, in a comparable manner to its quenching of cells labeled with FM.

Figure 3. Effects of temperature on the polarization of FepAS271C-FM and FepAS397C-FM. Bacteria were grown and fluorescently labeled, washed, and 5 x 10^7 bacteria were deposited into a 2 ml cuvette for polarization measurements. Polarization was deterimed at 4 ^{o}C, and at 500 s the temperature of the sample cuvette jacket was raised to 37 ^{o}C.

Figure 4. Transport of FeEnt by KDF541/pS271C-FM. The time courses of spectroscopic intensity change (**A)** and ^{59}FeEnt uptake (**B**) were compared in fluorescently labeled bacteria. The cells were suspended to 2.5 x 107 cells/ml in MOPS minimal media with glucose and casamino acids at 20 ^{o}C; for the fluorescence measurements, at t=0 FeEnt was added to 10 nM, and intensity changes were measured in the fluorescence spectrometer. In the radioactivity determinations, at t=0 ^{59}FeEnt was added to 10 nM, and aliquots were removed at the indicated times, filtered (o-o), and the filters were counted. The data monitor the accumulation of ^{59}FeEnt by the bacteria.

Figure 5. Effects of environmental conditions on the fluorescence time course. KDF541 (*tonB*$^{+}$)/pMF19/S271C was cultured in complete MOPS media (containing 0.4% glucose, 0.2% casamino acids, and supplementary auxotrophic amino acids), labeled with FM, and diluted to 2.5 x 10^{7} cells/ml in physiological buffers and different conditions. **A. Media.** The fluorescence response of the cells to 2 nM FeEnt (added at 300 s) was observed at 20 ^{o}C in complete MOPS media (green), or MOPS media without amino acids (teal), or TBS (blue); all media contained 0.4% glucose. The response of bacteria to which fluorescein was non-specifically adsorbed is also shown (black). KDF541/pMF19/pITS449 grown in LB for 14hrs, treated with FM as usual, and the fluorescence intensity of 5 x 10^{7} cells in 2 mL of MOPS media was monitored at 20 ^{o}C. FeEnt was added at 425sec. **B. Concentration, TonB-deficiency and pH.** Bacteria were diluted into complete MOPS media at 20 ^{o}C and pH 7.4, FeEnt was added (at 300 s) to 2 nM (green), 5 nM (teal), 10 nM (blue) or 20 nM (black), and

fluorescence intensity changes were recorded. KDF541/pMF19/S271C-AM was also tested in the same media with 2 nM FeEnt (magenta). The red curve derives from KDF571 (*tonB*) /pMF19/S271C-FM, subjected to the same regime in the same media; the grey curve derives from KDF541/pMF19/S271C-FM, tested in complete MOPS media that was adjusted to pH 4. **C. Temperature.** Bacteria were diluted into complete MOPS media and equilibrated at 20^{o}C (green), 15^{o}C (teal), 10^{o}C (blue) or 5^{o}C,(black). FeEnt was added to 10nM and the changes in fluorescence were recorded. The experiment was also performed with 2 nM FeEnt (inset) at 37 ^{o}C (magenta) or 20 ^{o}C (green).

Figure 6. Effects of metabolic poisons. In all panels, KDF541/pMF19/S271C was grown in complete MOPS media, labeled with FM, washed, and resuspended at 2.5 x 10^{7}/ml. **A. Energy poisons.** The labeled cells were suspended in MOPS media containing 0.4% glucose and shaken for 1 hour at 37^{o}C in the absence of any poison (green), or the presence of CCCP (0.1 mM, red), cyanide (20 mM, magenta), azide (10 mM, black), DNP (2 mM, blue) or arsenate (10 mM, teal). The cells were equilibrated at 20 ^{o}C, FeEnt was added to 2 nM (at 800 s), and fluorescence changes were monitored. **B. Carbon sources.** The cells were resuspended in MOPS media without glucose, shaken for 10 hours at 37 ^{o}C, equilibrated at 20 ^{o}C in the presence of 0.4% glucose (green), succinate (teal) ascorbate (blue), or the absence of an extraneous carbon source (black). FeEnt was added to 2 nM (at 1000 s) and fluorescence changes were monitored. **C. Arsenate and Phosphate.** Labeled cells were resuspended in MOPS media plus glucose and shaken for 1 hour at 37^{o}C in the absence of test compounds

(green), or the presence of 30 mM sodium phosphate (magenta); 30 mM sodium phosphate and 10mM sodium arsenate (blue), or 10 mM sodium arsenate (teal). The cells, in the same buffers, were re-equilibrated at 20°C, FeEnt was added to 2 nM (at 800 s), and fluorescence intensity changes were recorded.

References

1. Neilands, J. B. (1982) Annu Rev Microbiol 36, 285-309
2. Neilands, J. B. (1995) J Biol Chem 270(45), 26723-6
3. Rutz, J. M., Liu, J., Lyons, J. A., Goranson, J., Armstrong, S. K., McIntosh, M. A., Feix, J. B., and Klebba, P. E. (1992) Science 258(5081), 471-5
4. Wayne, R., and Neilands, J. B. (1975) J Bacteriol 121(2), 497-503
5. Wayne, R., Frick, K., and Neilands, J. B. (1976) J Bacteriol 126(1), 7-12
6. Di Masi, D.R. White, J.C., Schnaitman, C.A. and Bradbeer, C. (1973) J. Bacteriol. 115, 506-13.
7. Scott, D.C., Cao, Z. Qi, Z., Bauler, M, Igo, J.D., Newton S.M. and Klebba P.E. (2001) J. Biol. Chem. **276**:13025-33
8. Fiss E.H, Stanley-Samuelson P. and Neilands J.B. (1982) Biochemistry 31, 4517-22
9. Newton, S. M., Igo, J. D., Scott, D. C., and Klebba, P. E. (1999) Mol Microbiol 32(6), 1153-1165
10. Payne, M. A., Igo, J. D., Cao, Z., Foster, S. B., Newton, S. M., and Klebba, P. E. (1997) J Biol Chem 272(35), 21950-5
11. Cao, Z., Qi, Z., Sprencel, C., Newton, S. M., and Klebba, P. E. (2000) Mol Microbiol 37(6), 1306-17

12. Scott, D.C., Newton, S.M. and Klebba, P.E. (2002) J Bacteriol. **184**,4906-11

13. Ferguson, A.D., Chakraborty, R., Smith, B.S., Esser, L., van der Helm, D. and Deisenhofer, J. (2002) Science. **295**,1715-9

14. Jiang, X., Payne, M. A., Cao, Z., Foster, S. B., Feix, J. B., Newton, S. M., and Klebba, P. E. (1997) Science 276(5316), 1261-4

15. Cao, Z., Newton, S.M. and Klebba, P.E. *Submitted for publication.*

16. Wang, C. C., and Newton, A. (1971) J Biol Chem 246(7), 2147-51

17. Guterman, S.K. (1973) J. Bacteriol. 114, 1217-24

18. Guterman, S. K., and Dann, L. (1973) J Bacteriol 114(3), 1225-30

19. Wang, C.C. and Newton, A. (1969) J Bacteriol, **98**(3), 1142-50

20. Pugsley, A. P., and Reeves, P. (1976) J Bacteriol 127(1), 218-28

21. Reynolds, P. R., Mottur, G. P., and Bradbeer, C. (1980) J Biol Chem 255(9), 4313-9

22. Bradbeer, C. (1993) J Bacteriol 175(10), 3146-50

23. Nikaido, H., and Vaara, M. (1985) Microbiol Rev 49(1), 1-32

24 Nikaido, H., and Rosenberg, E.Y. (1981) J. Gen. Physiol. 77, 121-35

25. Nikaido, H., and Rosenberg E.Y. (1983) J. Bacteriol. 153, 241-52

26. Luckey, M., and Nikaido, H. (1980) Proc. Nat. Acad. Sci. U S A. 77, 167-71

27. Postle, K. (1993) J. Bioenerg. Biomembr. 25, 591

28. Letain, T.E. and Postle, K (1997) Mol. Microbiol. 24, 271

29. Klebba, P. E., and Newton, S. M. (1998) Curr Opin Microbiol 1(2), 238-247

30. Buchanan, S. K., Smith, B. S., Venkatramani, L., Xia, D., Esser, L., Palnitkar, M., Chakraborty, R., van der Helm, D., and Deisenhofer, J. (1999) Nat Struct Biol 6(1), 56-63

31. Locher, K. P., Rees, B., Koebnik, R., Mitschler, A., Moulinier, L., Rosenbusch, J. P., and Moras, D. (1998) Cell 95(6), 771-8

32. Ferguson, A. D., Hofmann, E., Coulton, J. W., Diederichs, K., and Welte, W. (1998) Science 282(5397), 2215-20

33. Liu, J., Rutz, J. M., Klebba, P. E., and Feix, J. B. (1994) Biochemistry 33(45), 13274-83

34. Klug C.S., Su W., Liu J., Klebba P.E., and Feix J.B. (1995) Biochemistry 31, 14230-6

35. Locher K.P., and Rosenbusch J.P. (1997) Eur J Biochem 247, 770-5

36. Armstrong, S.A, Francis, C.L., and McIntosh, M.A (1990) J. Biol. Chem. 265, 14536-14575

37. Feldman, M.F., and Valvano M.A. (1999) J. Biol. Chem. 274, 35129-38

38. Gibson F., Cox G.B, Downie J.A. and Radik J. (1977) Biochem. J. 162, 665-670

39 Klebba, P. E., McIntosh, M. A., and Neilands, J. B. (1982) J Bacteriol 149(3), 880-8

40. Pollack J.R., and Neilands J.B. (1970) Biochem. Biophys. Res. Commun. 38, 989-92

41. Murphy, C. K., Kalve, V. I., and Klebba, P. E. (1990) J Bacteriol 172(5), 2736-46

42. Newton, S. M., Allen, J. S., Cao, Z., Qi, Z., Jiang, X., Sprencel, C., Igo, J. D., Foster, S. B., Payne, M. A., and Klebba, P. E. (1997) Proc Natl Acad Sci U S A 94(9), 4560-5

43. Miller, J. H. (1972) Experiments in molecular genetics. Cold Spring Harbor Laboratory, Cold Spring Harbor, N.Y.

44. Neidhardt, F.C., Bloch, P.L., Smith, D.F. (1974) J. Bacteriol. 119: 736–747

45. Cao, Z (1999) Ph. D. Thesis, University of Oklahoma

46. Einstein, A (1906) Ann. Phys. 19, 371

47. Langevin, P. (1908) Comptes Rendues 146, 530

48. Leong, J., and Neilands, J.B. (1976) J. Bacteriol. 126, 823-831

49. Ecker, D., Matzanke, B. and Raymond, K.N. (1986) J. Bacteriol. 167, 666-675

50. Pugsley, A. P., and Reeves, P (1977) J. Bacteriol. 130, 26-36.

51. Thulasiraman, P., Newton, S. M., Xu, J., Raymond, K. N., Mai, C., Hall, A., Montague, M. A., and Klebba, P. E. (1998) J. Bacteriol. 180, 6689-96

52. Usher, K.C., Ozkan, E., Gardner, K.H. Deisenhofer, J. (2001) Proc. Natl. Acad. Sci. USA 98:10676-81.

53. Bos, C., Lorenzen, D., Braun, V. (1998) J. Bacteriol.180:605-13.

54. Schalk, I.J., Kyslik, P., Prome, D., van Dorsselaer, A., Poole, K., Abdallah, M.A., Pattus, F. (1999) Biochemistry 38:9357-65.

55. Schalk, I.J., Hennard, C., Dugave, C., Poole, K., Abdallah, M.A., Pattus, F. (2001) Mol. Microbiol. 9:351-60.

56. Schalk, I.J., Abdallah, M.A., Pattus, F. (2002) Biochemistry 41:1663-71.

57. Sprencel, C., Cao, Z., Qi, Z., Scott, D.C., Montague, M.A., Ivanoff, N., Xu, J., Raymond, K.M., Newton, S.M., Klebba, P.E. (2000) J. Bacteriol. 182:5359-64.

58. Pugsley A.P. and Reeves P. (1977) J. Bacteriol. 130, 26-36.

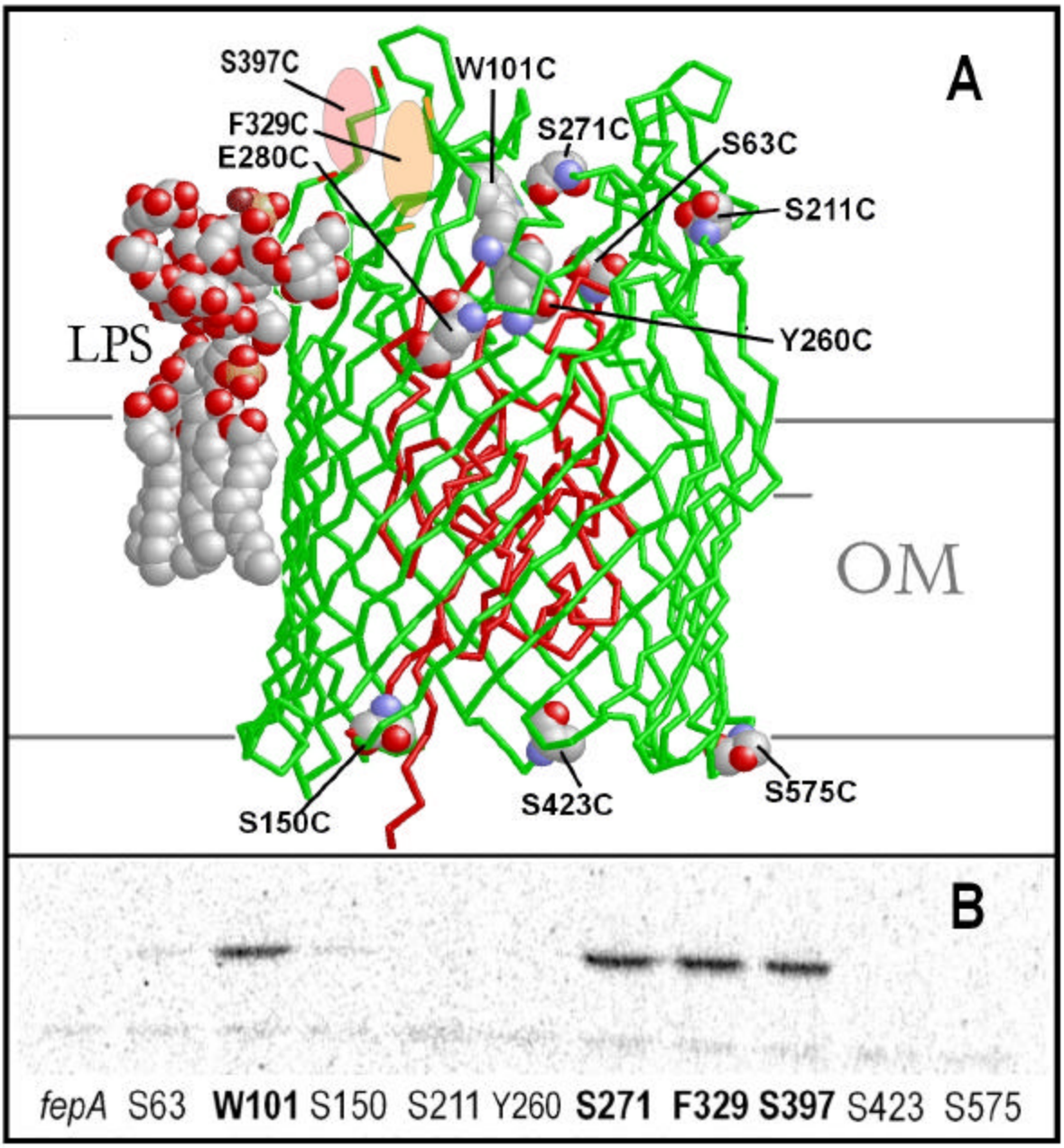
A
S397C
W101C
F329C
E280C
S271C
S63C
S211C
LPS
Y260C
OM
S150C
S423C
S575C
B
fepA S63 W101 S150 S211 Y260 S271 F329 S397 S423 S575

Figure 1

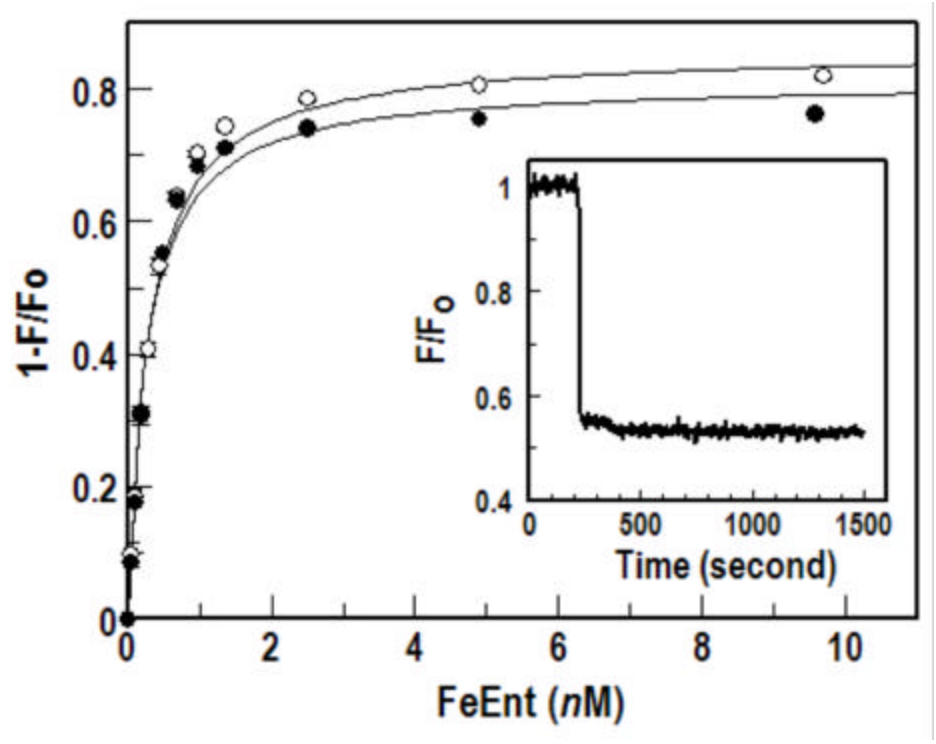

Figure 2

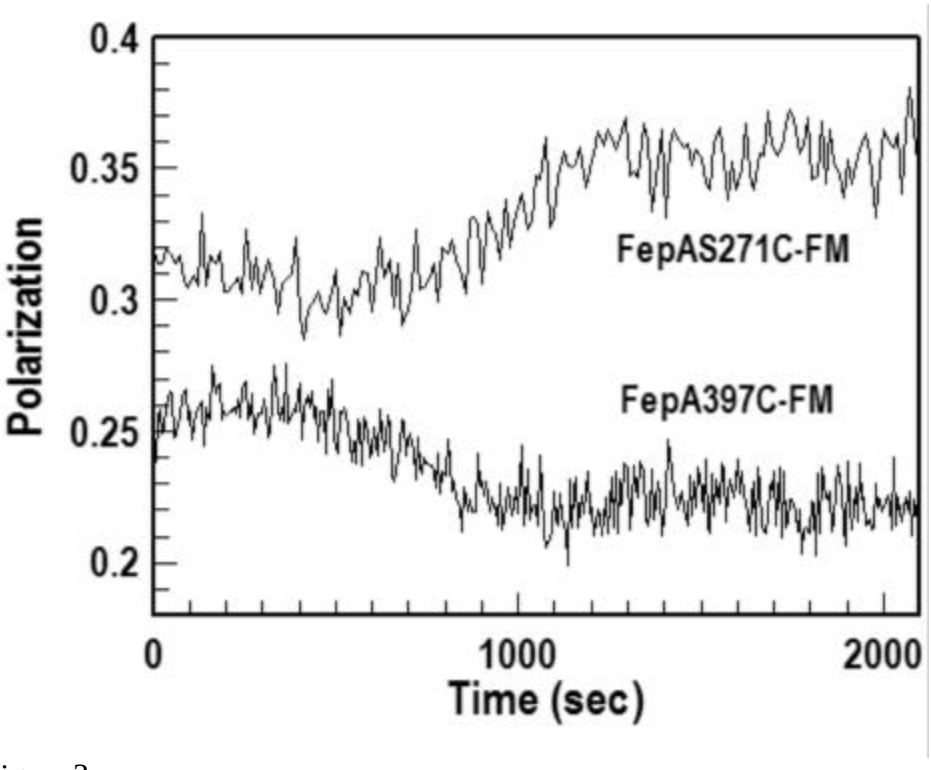

Figure 3

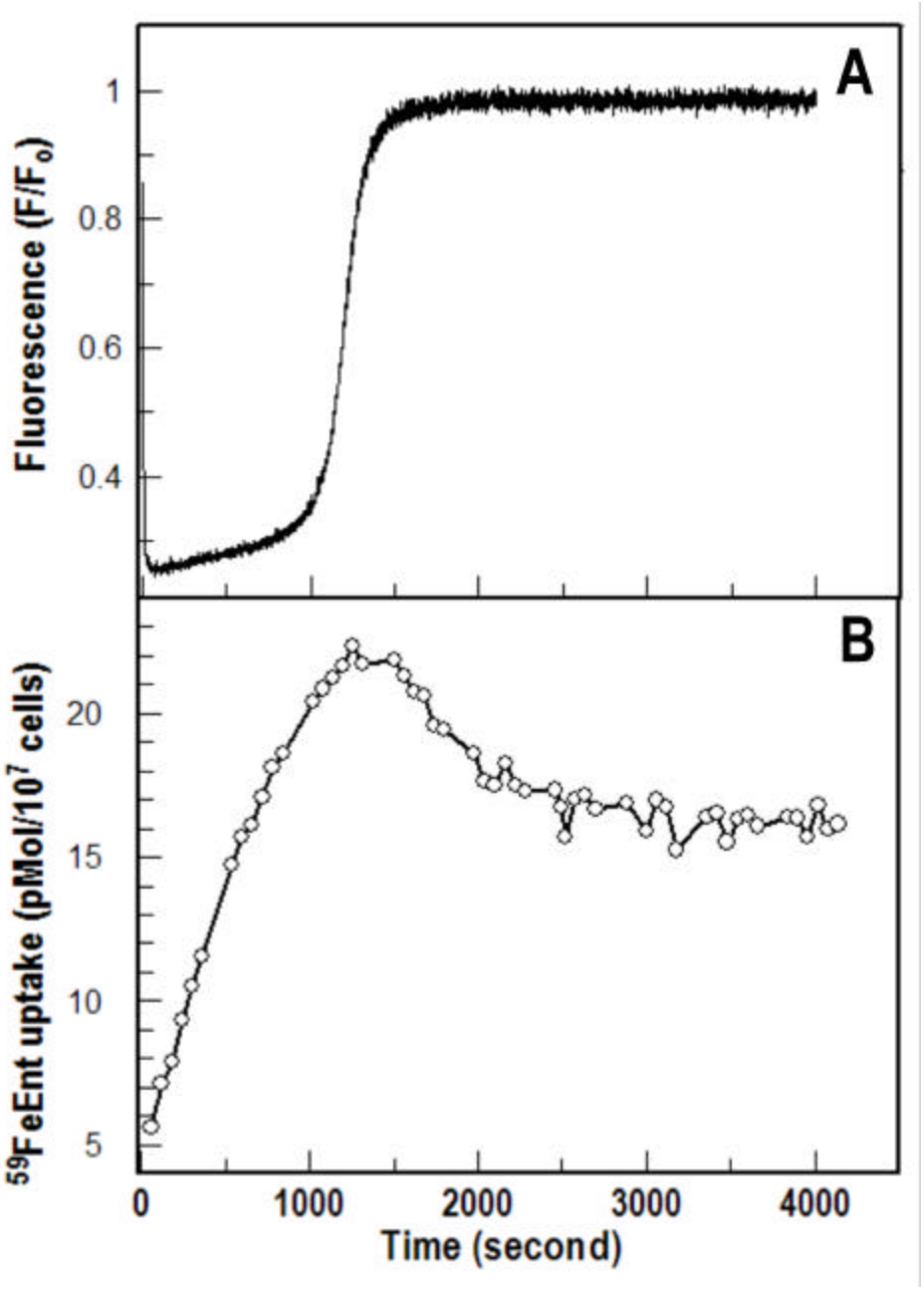
A
B
Fluorescence (F/F$_o$)
1
0.8
0.6
0.4
^{59}FeEnt uptake (pMol/10^7 cells)
20
15
10
5
0
1000
2000
3000
4000
Time (second)

Figure 4

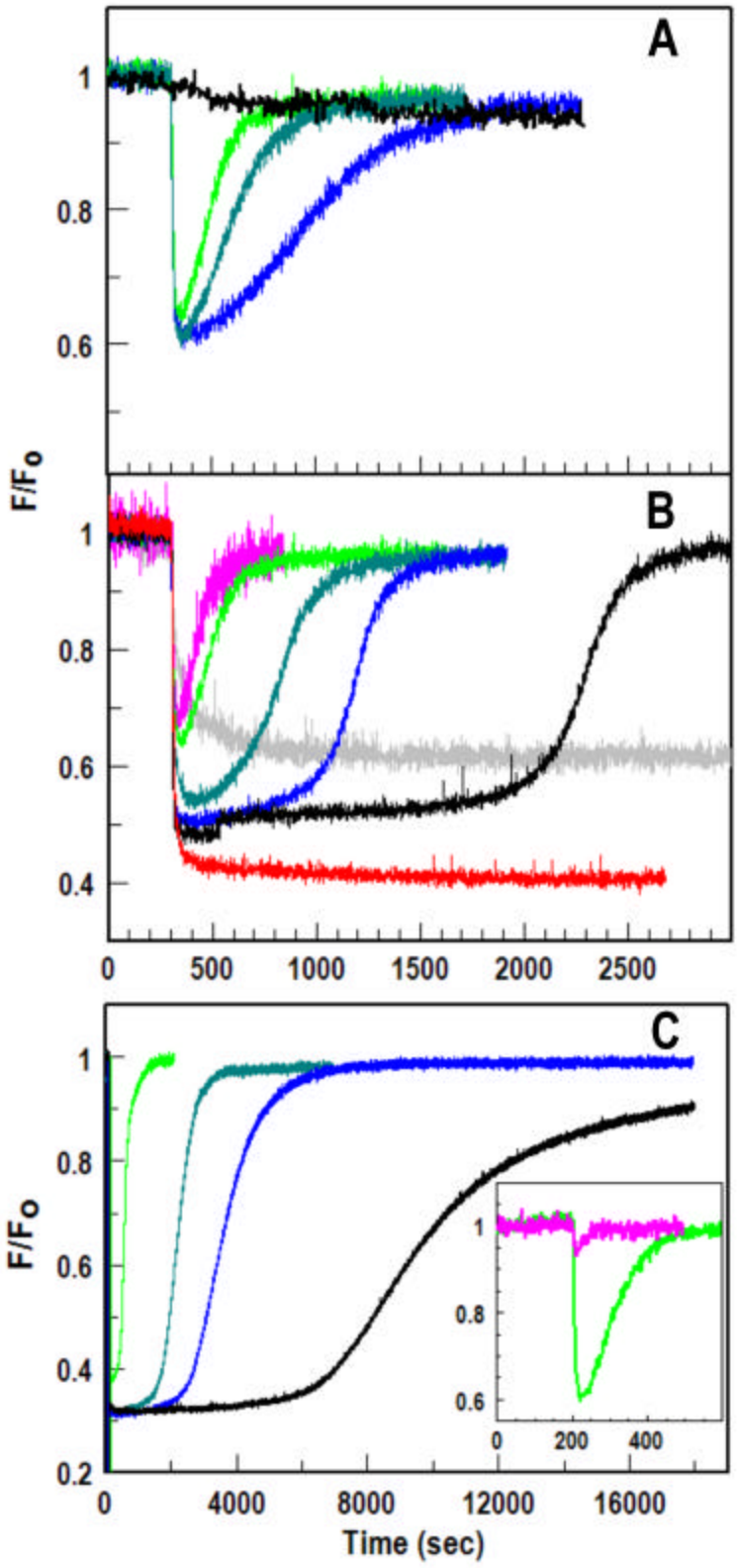
A
B
C
F/Fo
Time (sec)
1
0.8
0.6
0.4
0.2
0
500
1000
1500
2000
2500
4000
8000
12000
16000
200
400

Figure 5

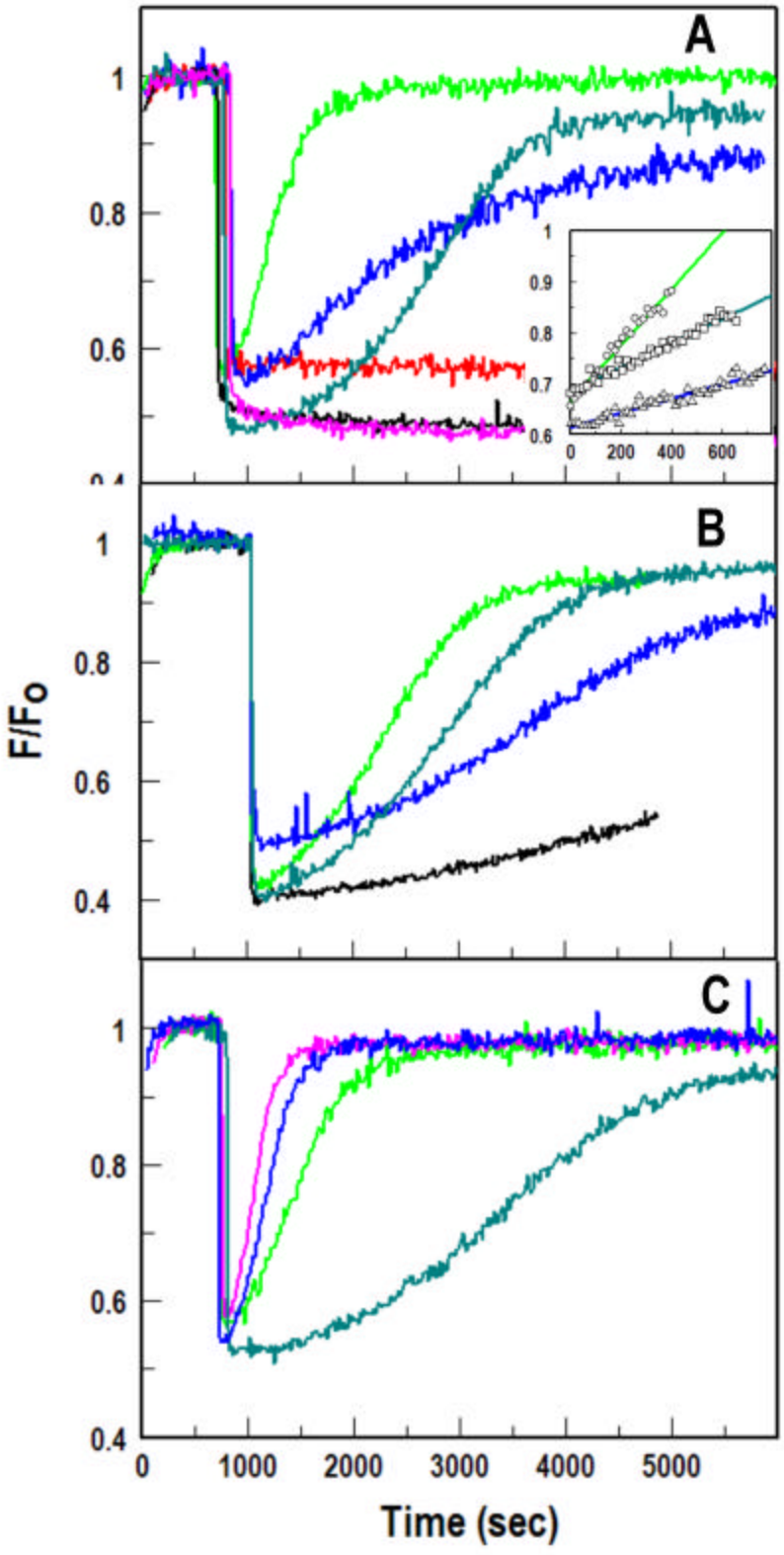
A
B
C
F/Fo
Time (sec)
1
0.8
0.6
0.4
0
1000
2000
3000
4000
5000
0.9
0.7
200
400
600

Figure 6